Enhancement of Terahertz Emission using AuGe nano-patterns

Harshad Surdi[1], Abhishek Singh[1], and S.S.Prabhu[1]
[1]Tata Institute of Fundamental Research, Homi Bhabha Road, Mumbai, 400005, India
harshad.surdi@tifr.res.in, asingh@tifr.res.in, prabhu@tifr.res.in

Abstract: In this paper we have attempted to increase the emission efficiency of terahertz (THz) Photo-Conductive Antenna (PCA) by nano-patterning it with Gold Germanium (AuGe) nano-patterns. Nano-patterns with optimized geometrical features for specific optical frequency tend to excite localized surface plasmon resonance which cause localized electric field enhancement. This localized field enhancement causes an increase in the number of generated photo-carriers which increase the THz emission power by a factor of 4. COMSOL simulations give the approximate height (40nm) of these nano-patterns at which excitation of localized surface plasmon polaritons is the strongest.

Keywords: Terahertz, photoconductive antenna, surface plasmon polaritons, nano-patterns

1. Introduction

Terahertz (10^{12} Hz) technology lies on the grounds where electronics and optics come together. With the advent of terahertz technology, many attempts have been made to increase the efficiency and emission power of Terahertz Photo-Conductive Antennas (PCA). There have been many such successful attempts like employing microlens arrays [1], increasing effective length of electrodes [2], plasmonic contact electrodes [3], optical nanoantennas [4] etc. Terahertz technology has found various applications ranging from nondestructive imaging [5] to fingerprinting biological moleculees [6]. Time resolved terahertz spectroscopy is used to find optical constants of materials which are transparent or translucent at terahertz frequencies [7].

The field of nano-plasmonics exploits the light-matter interaction at nano-meter scale to increase the coupling of incident light. As a consequence it finds interesting applications in terahertz technology. With nanometer scale lithography techniques, nanometer sized metal structures with optimized geometrical features can be fabricated on dielectric interfaces to exactly match the resonant conditions to excite surface plasmon polaritons. At these particular conditions, local enhancement of field is observed at the metal-dielectric interface.

Our work exploits this local field enhancement nature of SPP in increasing the THz pulse power and hence giving more efficient THz antennas.

2. Theory

2.1 THz antenna structure and working

A terahertz PCA consists of a SI-GaAs substrate on which two AuGe electrodes are deposited with a separation of 20μm. The nano-patterns are AuGe squares having a diagonal of 500nm and a period of 600nm. These nano-patterns are incorporated in the THz antenna on the SI-GaAs region between the two electrodes. An ultrashort (10 femto-second) pulsed laser of 800nm and approximately 100mW average power is focused on the region between the AuGe electrodes. A dc bias of 20V is also applied at the electrodes [Fig. 2]. The photo-carriers generated by the laser pulse are accelerated towards the electrodes due to the dc bias. This acceleration of the photo-carriers induces the photo-current and produces the electromagnetic radiation in the terahertz region.

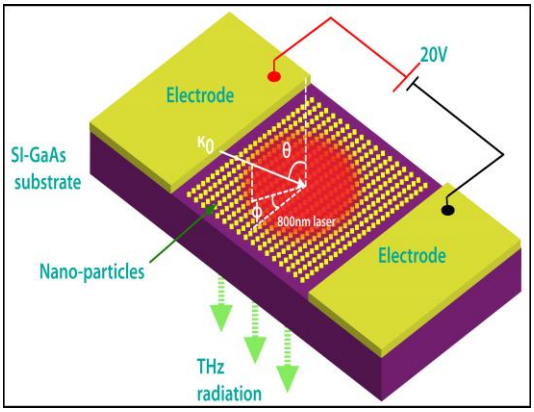

Figure 1: THz photo-conductive antenna incorporated with AuGe nano-patterns. A 20V dc is applied across the electrodes.

2.2. Fabrication

A bare SI-GaAs wafer is sputtered with AuGe in a sputter deposition chamber. The deposition is controlled to limit the thickness of the AuGe layer. The AuGe sputtered SI-GaAs is then spin-coated with a positive E-beam resist. Electron beam (E-beam) lithography (Raith) is used for patterning the resist on the AuGe layer. This patterning of the E-beam resist will act like a stencil of the shape of the nano-dots incorporated THz antenna. Several attempts of E-beam lithography, each with varying doses ($\mu C/cm^2$) of the electron beam, have to be performed to obtain the dimensions of the nano-dots closest possible to their expected dimensions. The complete antenna structure can then be obtained by etching out the unwanted AuGe according to the 'stencil' using Reactive Ion etching.

2.2. Surface Plasmon Polaritons

Surface Plasmon Polaritons (SPPs) are electromagnetic excitations propagating at the metal-dielectric interface confined to a perpendicular direction. SPPs are a result of the coupling of the incident light's electromagnetic field to the oscillations of the metal's electron plasma. They follow the following dispersion relation

$$\kappa_{SPP} = \kappa_0 \sqrt{\frac{\varepsilon_a \varepsilon_b}{\varepsilon_a + \varepsilon_b}}$$

Where κ_{SPP} is the momentum of the SPP, κ_0 is the free space wave vector $\left(\kappa_0 = \left(\frac{\omega}{c}\right)\right)$, $\varepsilon_a, \varepsilon_b$ is the relative permittivity of media *a* and *b*. As we can see from the equation, κ_{SPP} is greater than κ_0. This means we should compensate for the extra momentum in order to excite SPPs from air.

The metallic grating provides an extra momentum along the direction of the grating. Hence, to excite SPP, the condition to be satisfied should be

$$\kappa_{SPP} = \kappa_0 \sqrt{\frac{\varepsilon_a \varepsilon_b}{\varepsilon_a + \varepsilon_b}} = \kappa_0 \sin\theta + \vec{G}$$

where

$\vec{G} = \frac{2\pi}{\Lambda}$, Λ being the grating period

But for a normal incidence θ is zero and hence the equation becomes

$$\kappa_0 \sqrt{\frac{\varepsilon_a \varepsilon_b}{\varepsilon_a + \varepsilon_b}} = \frac{2\pi}{\Lambda}$$

Hence from the equation we can calculate the grating period needed to excite SPP.

With the excitation of the SPP, local electric field is enhanced which in turn produces larger number of photo-carriers. The increase in number of photo-carriers increases the THz emission.

3. Use of COMSOL

For the simulation of SPP, the "Electromagnetic Waves, Frequency Domain" interface of the Wave Optics Module was used. A 2D simulation as well as a 3D simulation was done to optimize the resonance conditions for strong excitations of SPP. In both the simulations, the complete structure consists of three domains viz. air, AuGe nano-patterns and GaAs substrate [Fig. 2 (a), (b)]. In the 3D simulation, PMLs of 150nm thickness surrounded both air and substrate domains. Two Port nodes were used; first port to launch the light plane wave with propagation constant as that of air and second port to absorb the transmitted plane wave with propagation constant as that of the GaAs substrate. Floquet periodic boundary conditions were used so as to limit the simulation to a single periodic element. The local wave vector and the direction of the incident electric field vector are used as input parameters to the ports and the Floquet periodic conditions.

For the 3D simulation, sweep meshing for the air and substrate domains and free tetrahedral with extremely fine element size was used. For the 2D simulation, all the domains were meshed with free triangular mesh with extremely fine element size. MUMPS direct solver with increased "out-of-core" memory was used to solve both the simulations since iterative solvers

would fail to converge to a solution. This may be because of large number of degrees of freedom.

A parametric sweep of the frequency as well as the height of the nano-patterns was done. The frequency parameter sweep emulates the band of frequencies pulsed laser used experimentally. The height sweep of the nano-patterns gives a fair idea of the optimized height at which the excitation of SPP is strongest.

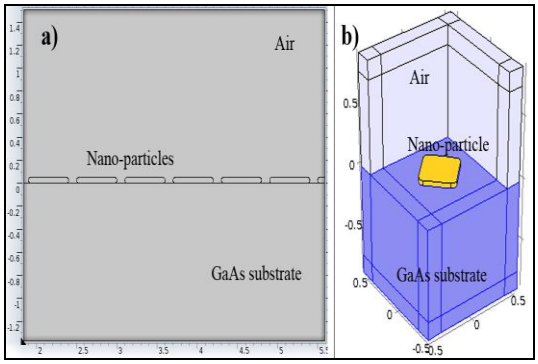

Figure 2: (a) 2D Simulation CAD **(b)** cut-out of 3D simulation CAD. A single nano-pattern is 500nm diagonally and is separated by 100nm from adjacent nano-patterns.

5. Governing Equations

Considering spherical coordinate system **[Figure 1]** the wave vector is

$$\kappa_p = (\kappa_x, \kappa_y, \kappa_{pz}) = \kappa_p(\cos\phi_p \sin\theta_p, \sin\phi_p \sin\theta_p, -\cos\theta_p)$$

Where *p = a (air), b (substrate)*; ϕ *and* θ are azimuthal and polar angles of incidence and κ_p is the wave vector in that medium. With normal incidence of the plane wave the wave vectors become

$$\kappa_a = \kappa_{az} = -\kappa_a \text{ and } \kappa_b = \kappa_{bz} = -\kappa_b$$

Also,

$$\kappa_b = \frac{n_b}{n_a}\kappa_a,$$

$$\phi_b = \phi_a,$$

$$\sin\theta_b = \frac{n_a}{n_b}\sin\theta_a$$

The polarized electric field vector at the plane of incidence becomes

$$\mathrm{E}_0 = E_0 \exp(-i(\kappa_x x + \kappa_y y))$$

The electric field at absorption port will then be proportional to

$$\exp(\text{-i}(\kappa_x x + \kappa_y y))$$

To solve for the electric field in all the media, the 'Electromagnetic Wave, Frequency Domain' interface uses the wave equation which follows from the Maxwell's Equations.

$$\nabla \times \mu_r^{-1}(\nabla \times E) - \kappa_0^2(\varepsilon_r - \frac{j\sigma}{\omega\varepsilon_0})E = 0$$

Where E is the electric field, ω is the angular frequency, ε_r is the relative permittivity, μ_r is the relative permeability and σ is the electrical conductivity.

6. Results and Discussion

The parametric sweep of the height of the nano-patterns reveals that at 40nm the excitation of SPP is strongest [Fig. 3].

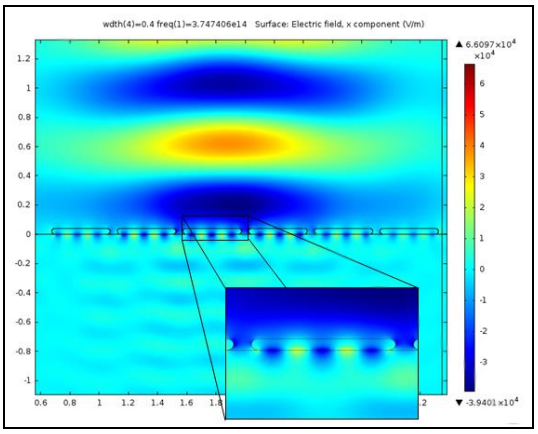

Figure 3: 2D simulation results. Enhancement in the electric field beneath the nano-pattern is observed as an indication of excitation of SPP for a height of 40nm of the nano-patterns.

Also from the 3D simulation we can observe the increase in the electric field just beneath the nano-pattern at its edges [Fig 4].

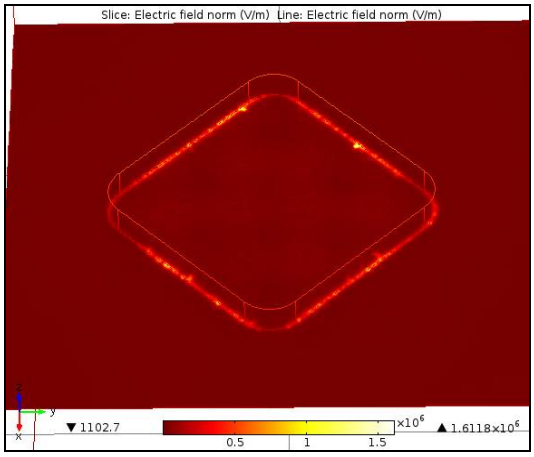

Figure 4: 3D simulation results show the field enhancement at the nano-pattern-GaAs interface on the edges of the nano-pattern

The THz antenna incorporated with nano-patterns was fabricated [Fig. 5] and tested for THz generation. It is clear from the comparison in Fig. 6 that the signal of the THz antenna with nano-patterns is approximately two times that of the THz antenna without the nano-patterns. Also the spectrum of the two antennas is the same, as is evident from the FFT as shown in Fig. 7. Also we can say that the power of the THz antenna has increased fourfold.

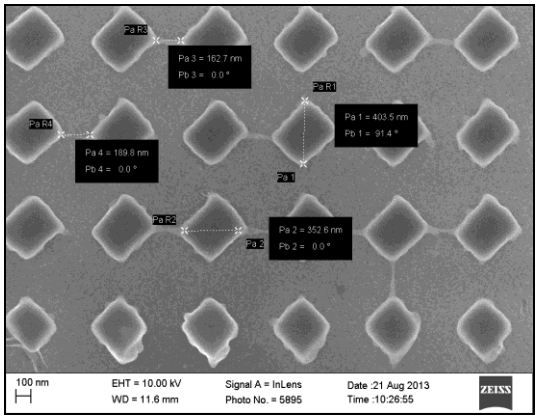

Figure 5: SEM image of AuGe nano-patterns on SI-GaAs substrate.

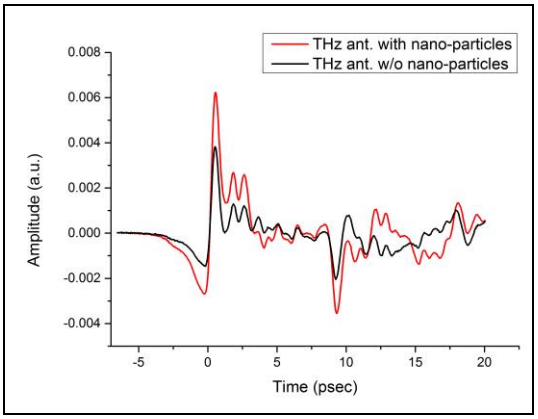

Figure 6: Time domain signals of the THz antenna with and without the nano-patterns. Approximately a two-fold increase in the amplitude is seen.

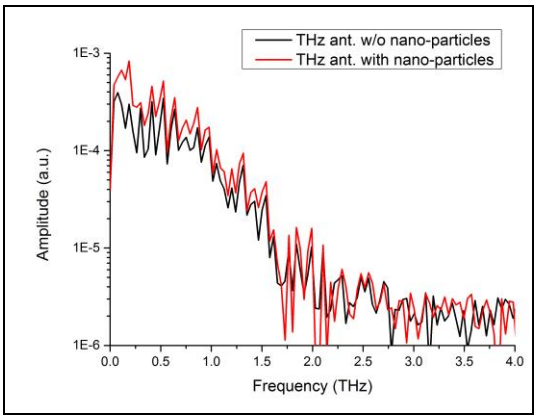

Figure 7: Frequency domain signals of the THz antenna with and without the nano-patterns. There seems to be no significant change in he spectrum.

7. Conclusion

The resonant condition for excitation of SPP is solely governed by the geometry of the grating (in this case the nano-patterns). COMSOL simulations confirmed the geometrical features required of the nano-patterns to excite the strongest SPP. The excitation of SPP leads to the local enhancement in the electrical field which increases the generation photo-carriers and thereby increasing the THz emission power by a factor of 4.

8. References

1. G. Matthaus, et. al. "Large-area microlens emitters for powerful THz emission", *Appl. Phys. Lett.*, **Vol. B96**, pp. 233-235 (2009)

2. Abhishek Singh, Harshad Surdi, V. V. Nikesh, S. S. Prabhu, G. H. Döhler, "Improved Efficiency of Photoconductive THz Emitters by Increasing the Effective Contact Length of Electrodes" , *arxiv.org/abs/1306.6780*

3. Sang-Gil Park, Kyong Hwan Jin, Minwoo Yi, Jong Chul Ye, Jaewook Ahn, and Ki-Hun Jeong, "Enhancement of Terahertz Pulse Emission by Optical Nanoantenna", *ACS Nano,* **Vol. 6 (3)**, *pp. 2026–2031*(2012)

4. C. W. Berry, N. Wang, M. R. Hashemi, M. Unlu, M. Jarrahi, "Significant Performance Enhancement in Photoconductive Terahertz Optoelectronics by Incorporating Plasmonic Contact Electrodes", *Nature Communications*, **Vol. 4, 1622** (2013)

5. Kodo Kawase, Yuichi Ogawa, Yuuki Watanabe, and Hiroyuki Inoue, "Non-destructive terahertz imaging of illicit drugs using spectral fingerprints", *Optics Express*, **Vol. 11, Issue 20**, pp. 2549-2554 (2003)

6. Walther, M., Plochocka, P., Fischer, B., Helm, H. and Uhd Jepsen, P., "Collective vibrational modes in biological molecules investigated by terahertz time-domain spectroscopy". *Biopolymers*, **Vol. 67**, pp. 310–313 (2002)

7. Shen, Y. -C; Lo, T.; Taday, P.F.; Cole, B.E.; Tribe, W.R.; Kemp, M.C., "Detection and identification of explosives using terahertz pulsed spectroscopic imaging," *Applied Physics Letters* , **Vol. 86, no.24**, pp.241116,241116-3, (2005)

8. Stefan Alexander Maier, Plasmonics: Fundamentals and Applications XXV, 5-19pg (2007)